Minipig model of Huntington´s disease: ^{1}H magnetic resonance spectroscopy of the brain

Maria Jozefovicova[1]*, Vít Herynek[1], Filip Jiru[1], Monika Dezortova[1], Jana Juhasova[2], Stefan Juhas[2], Jan Motlik[2], Milan Hajek[1]

[1]MR Unit, Department of Diagnostic and Interventional Radiology, Institute for Clinical and Experimental Medicine, Videnska 1958/9, 14021, Prague, Czech Republic

[2]Institute of Animal Physiology and Genetics, Academy of Sciences, Rumburska 89, 277 21, Libechov, Czech Republic

*Permanent address: Department of NMR Spectroscopy and Mass Spectroscopy, Faculty of Chemical and Food Technology, Slovak University of Technology, Radlinského 9, 812 37, Bratislava, Slovak Republic

Corresponding author:

Vit Herynek

MR Unit, Department of Diagnostic and Interventional Radiology

Institute for Clinical and Experimental Medicine

Videnska 1958/9, 14021, Prague, Czech Republic

e-mail: vit.herynek@medicon.cz

Phone: +420 26136 2703

Short title:

Minipig model of Huntington´s disease: ^{1}H MRS of the brain

The results were presented in part at the scientific meeting of the European Society for Magnetic Resonance in Medicine and Biology, Toulouse, France, October 3–5, 2013.

Summary

Huntington's disease (HD) is an inherited autosomal neurodegenerative disorder affecting predominantly the brain, characterized by motor dysfunctions, behavioral and cognitive disturbances. The aim of this study was to determine changes in the brain of transgenic minipigs before HD onset using ^{1}H magnetic resonance (MR) spectroscopy.

Measurements were performed on a 3T MR scanner using a single voxel spectroscopy sequence for spectra acquisition in the white matter and chemical shift imaging sequence for measurement in the striatum, hippocampus and thalamus.

A decrease of (phospho)creatine (tCr) concentration was found only in the thalamus (p=0.002) of transgenic minipigs, nevertheless we found significant changes in metabolite ratios. Increase of the ratio choline compounds (tCho)/tCr was found in all examined areas: striatum (p=0.010), thalamus (p=0.011) as well as hippocampus (p=0.027). The ratio N-acetylaspartate+N-acetylaspartylglutamate (tNAA)/tCr (p=0.043) and glutamate+glutamine (Glx)/tCr(p=0.039) was elevated in the thalamus, the ratio myo-inositol (Ins)/tCr (p=0.048) was significantly increased in the hippocampus.

No significant differences were observed in the metabolite concentrations in the white matter, however we found significant increase of ratios tNAA/tCr (p=0.018) and tCho/tCr (p=0.003) ratios in transgenic boars.

We suppose that the majority of the observed changes are predominantly related to changes in energy metabolism caused by decrease of tCr.

Keywords

Huntington´s disease; Minipigs; Magnetic resonance spectroscopy; Brain; Metabolite concentrations

Abbreviations:

2D-CSI two-dimensional chemical shift imaging

DTI diffusion tensor imaging

FOV field of view

Glx glutamate+glutamine

HD Huntington's disease

HTT huntingtin gene

Ins myo-inositol

MR magnetic resonance

MRS magnetic resonance spectroscopy

NAA N-acetylaspartate

NA number of acquisitions

PRESS point resolved spectroscopy

ROI region of interest

SVS single voxel spectroscopy

tCho choline compounds

tCr (phospho)creatine

TE echo time

TgHD transgenic HD

tNAA N-acetylaspartate+N-acetylaspartylglutamate

TR repetition time

VOI volume of interest

WM white matter

Introduction

Huntington's disease (HD), an inherited autosomal neurodegenerative disorder, affects predominantly the brain. Clinical manifestations are motor dysfunctions, behavioral and cognitive disturbances. It is caused by an unstable CAG (cytosine–adenine–guanine) expansion in the huntingtin gene (HTT) on the short arm of chromosome 4. The disease fully develops when the exon-1 of HTT gene contains more than 40 CAG repeats, whereas an intermediate number (36–40) of trinucleotides leads to a slower progression of the pathology. The number of CAG repeats inversely correlates with the onset and severity of this disease, however, the precise function of the trinucleotide stretch remains unclear (Bano *et al.* 2011, Heikkinen *et al.* 2012, van den Bogaard *et al.* 2011).

Animal models play crucial roles in understanding pathological mechanisms and in the nature of neurodegeneration in HD and are important for developing therapeutic measures. Determination of symptom-independent biomarkers of HD neuropathology represents a key task for research, as they may predict disease evolution before its onset (Bohanna *et al.* 2008, Perez-De La Cruz and Santamaria 2007).

A large number of rodent models that have various degrees of similarity to the human HD pathology have been developed. From the different transgenic models available, R6/1 and R6/2 mice are most widely studied (Perez-De La Cruz and Santamaria 2007, Zuccato *et al.* 2010). However, the small size of the rodent brain and differences in neurostructure compared to humans limit their application for detailed neuroanatomical characterization (Baxa *et al.* 2013). To overcome these problems, larger HD genetic models such as the sheep, minipig, and the non-human primate have been developed (Morton and Howland 2013, Zuccato *et al.* 2010) The minipig is a suitable species due to big size of gyrencephalic brain and long lifespan. Moreover, there is a 96% similarity between the porcine and human huntingtin genes (Baxa *et al.* 2013).

Studies of HD in humans have revealed extensive changes throughout the brain (Bohanna *et al.* 2008). Nevertheless it is still not clear which structures are affected at different disease stages predominantly before the onset of the disease (van den Bogaard *et al.* 2011).

Magnetic resonance spectroscopy (MRS) is a non-invasive method used in research and clinical praxis that allows an evaluation of *in vivo* metabolism at the molecular level (Sundgren *et al.* 2005). By using ^{1}H MRS concentrations of metabolites N-acetylaspartate, creatine, phosphocreatine, glutamate, glutamine, choline-containing compounds, inositol, γ-aminobutyric acid and others can be determined (van den Bogaard *et al.* 2011).

^{1}H MRS has previously been considered as a biomarker method in premanifest and early states of HD (Sturrock *et al.* 2010). To evaluate *in vivo* brain metabolite differences mainly single voxel spectroscopy (SVS) has been used (Sturrock *et al.* 2010, Tkac *et al.* 2012, Zacharoff *et al.* 2012), but several studies have also used two-dimensional chemical shift imaging (2D-CSI) (Reynolds *et al.* 2005, Rotondo *et al.* 2003, Sundgren *et al.* 2005).

Studies measuring changes by MRS revealed different results for metabolite concentrations in patients with HD (Sturrock *et al.* 2010, van den Bogaard *et al.* 2011, van Oostrom *et al.* 2007). Various changes in metabolite concentration have also been found in different animal models that try to reflect the human HD condition (Jenkins *et al.* 2005).

The aim of this study was to determine changes in the brain of transgenic HD (TgHD) minipigs (model according to (Baxa *et al.* 2013)) before HD onset.

To investigate different regions of the brain we used SVS and 2D-CSI MRS. The ability of 2D-CSI technique to determine metabolite changes in various brain regions (striatum, thalamus, and hippocampus) enabled detailed diagnostics of possible brain pathologies in this HD minipig model, whereas SVS was used to obtain information from a substantial part of the white matter (WM). These data could provide a baseline for future MRS at clinical stage.

Materials and Methods

Minipigs

Minipigs came from the Institute of Animal Physiology and Genetics (Libechov, Czech Republic) where they were bred. The used strain is a result of a cross-breeding of strains from Minnesota (USA), Goettingen (Germany), and domestic farm strains. Successful germ line transmission occurred through successive generations (F0, F1, F2 and F3 generations) of a HD transgene encoding the first 548 aa of HTT with 124 glutamines under the control of human HTT promoter (Baxa *et al.* 2013). Until now several phenotypes have been detected in these TgHD minipigs expressing human mutated huntingtin. Some of these are: the reduced male reproductive parameters (e.g. fewer spermatozoa per ejaculate), impaired mitochondrial function in spermatozoa (Macakova *et al.* 2012) and blood serum cytokine imbalance (Benova *et al.* 2012). The founder sow (aged 5.5 years at the time of the study) as well as the offsprings are without clinical symptoms of HD at this point in time. We expect the outbreak of the clinical symptoms in the second half of their life, i.e., after the 10^{th} year. In this study transgenic minipigs from F2 generation before HD onset (N=7, male, 2 years old) and control siblings (N=6, male) were used. Their weight was 60-80 kg.

Minipigs were premedicated with intramuscular TKX mixture (Tiletaminum 5 mg/kg, Zolazepamum 5 mg/kg, Ketaminum 5 mg/kg, Xylazine 1 mg/kg) in combination with diazepamum (0.25 mg/kg, Apaurin). Anesthesia was maintained by intravenous administration of propofolum (Propofol 1% Fresenius) and TKX mixture. A pulse oximeter attached to a tail was used for continuous monitoring of minipig´s oxygen level in the blood and the pulse rate.

All experiments were performed with the approval of the State Veterinary Administration of the Czech Republic and according to current Czech regulations and guidelines for animal

welfare which comply with European Communities Council Directive of 24 November 1986 (86/609/EEC).

MRS experiments

Measurements were performed on a whole body 3 T MR scanner (Siemens Magnetom Trio) using a Tx/Rx head coil. For spectra localization, three perpendicular T2-weighted turbo spin echo images (repetition time/echo time TR/TE = 4400/99 ms, 4 mm slice thickness) were used. Point resolved spectroscopy (PRESS) - SVS sequence (TR/TE=5000/30 ms, volume of interest VOI=25x20x5 mm, number of acquisitions NA=96, acquisition time 8 min) was used for spectra acquisition in the WM. 2D-PRESS-CSI sequence (TR/TE=1510/30 ms, Field of view (FOV)=90x90x5 mm, VOI=30x30x5 mm, matrix=16x16, nominal voxel size 5.6x5.6x5.0 mm, the real voxel size measured as the FWHM (full width at half maximum) of the corresponding point spread function 8.3x8.3x5.0 mm, NA=32 (16x16x32 excitations using Hamming acquisition weighting), acquisition time 39 min 40 sec) was used for measurement in the striatum, hippocampus, and thalamus. The positioning of the SVS voxel and the 2D-CSI spectroscopic grid are shown in Fig.1. The homogeneity of the magnetic field was adjusted automatically based on B_0 mapping using a gradient echo sequence followed by the manual shimming when necessary. Outer volume suppression was used to avoid undesired signals from areas close to borders of the spectroscopic grid. For quantification of metabolites additional spectra without water suppression and with the same parameters, except for one acquisition, were obtained.

MRS post-processing

CSI spectra were analyzed using a program jSIPRO (Jiru *et al.* 2013) with implemented LCModel (Provencher 1993). CSI spectra pre-processing involved k-space Hamming filtering and zero filling to a 32x32 matrix resulting in the interpolated voxel size 2.8x2.8x5.0 mm. For quantification of SVS and CSI spectra LCModel basis set included 18 metabolites as well as

simulated signals of lipids and macromolecules. Signals of N-acetylaspartate+N-acetylaspartylglutamate (tNAA), (phospho)creatine (tCr), choline compounds (tCho), glutamate+glutamine (Glx), and myo-inositol (Ins) were quantified. Unsuppressed water signal served as an internal reference for the metabolite quantification.

Default LCModel water concentration (LCModel parameter: WCONC=35880 mmol/kg) and relaxation times (LCModel parameter: attenuation factor ATTH2O=0.7) for the human brain were used for the calculation of metabolite concentrations. Absolute concentrations of the metabolites were expressed as mmol/kg tissue. The ratios of metabolites to tCr were also determined.

Statistics

For the statistical evaluation only spectra with all evaluated metabolites (tNAA, tCr, tCho, Glx, Ins) having Cramér–Rao lower bound reported by LCModel below 20% were used. This criterion was fulfilled for spectra from 6 HD (SVS) and 5 HD (2D-CSI) and from 6 control (SVS, 2D-CSI) minipigs which were used for further quantification.

The resulting representative concentration of each metabolite measured by 2D-CSI was determined as an average of the concentration values obtained from the spectra of 3-6 voxels (matrix 32x32) in each analyzed area (striatum, thalamus and hippocampus).

The data for each metabolite, or for each metabolite to tCr ratio, was tested for normal distribution (Shapiro - Wilk test) and homogeneity of variance (Levene's tests - absolute and squared deviations) resulting in the confirmation of null hypothesis. The differences between groups were evaluated using two-tailed Student’s t-test and $p < 0.05$ was considered as a statistically significant difference. Corrections for multiple comparisons were not used, as they are not recommended when the study focuses on only a few scientifically sensible comparisons.

Results

White Matter

Metabolite concentrations in the white matter were measured using SVS. Examples of typical spectra from WM (HD and control) are shown in Fig. 2. The average values of the absolute concentrations of five metabolites (tNAA, tCr, tCho, Glx, Ins) and their ratios to tCr are summarized in Table 1. No significant differences were observed in the metabolite concentrations alone, however, significant increases of tNAA/tCr ($p=0.018$) and tCho/tCr ($p=0.003$) ratios were found in TgHD animals.

Striatum, thalamus, hippocampus

Changes of metabolite concentrations in the striatum, thalamus and hippocampus were determined by the 2D-CSI sequence. Typical spectra from the thalamus in HD and control minipigs are shown in Fig. 3. As in the case of SVS, five metabolites (tNAA, tCr, tCho, Glx, Ins) have been quantified. Metabolite concentrations and their ratios to tCr in the striatum, thalamus and hippocampus are summarized in Table 2.

The only significant change in metabolite concentration was a decrease in tCr in the thalamus ($p=0.002$) of transgenic boars, nevertheless we found significant changes in metabolite ratios. Increase of the ratio tCho/tCr was found in all examined areas: striatum ($p=0.010$), thalamus ($p=0.011$) as well as hippocampus ($p=0.027$). The ratios tNAA/tCr ($p=0.043$) and Glx/tCr($p=0.039$) were elevated in the thalamus, the ratio Ins/tCr ($p=0.048$) was significantly increased in the hippocampus.

Discussion

Huntington disease is accompanied by severe changes on a cellular level manifested also by metabolic changes in the brain tissue, however, little is known about the changes before clinical symptoms occur. Therefore we set out to determine changes in the brain metabolites

of control and transgenic minipig before the onset of HD. MRS represents an interesting tool for investigation of these preclinical changes *in vivo*.

Two recent ^{1}H MRS studies in HD patients, one at 3 T (Sturrock *et al.* 2010) and the other one at 7 T (van den Bogaard *et al.* 2011), found significant differences in neurochemical profile of HD brain only after the manifestation of clinical symptoms (Henry and Mochel 2012). Nevertheless an earlier study at a lower magnetic field of 0.5 T showed some changes of metabolite concentration in premanifest HD (Reynolds *et al.* 2005).

Van den Bogaard et al. demonstrated lower levels of N-acetylaspartate (NAA), creatine and Glx in putamen and decreased concentration of NAA and creatine in caudate nucleus (van den Bogaard *et al.* 2011). Sturrock et al. published decreased NAA, glutamate and tCr, increased tCho and Ins levels in putamen (Sturrock *et al.* 2010). Another study found decreased total choline concentration in frontal cortex (Gómez-Ansón *et al.* 2007).

We determined metabolite changes in WM and hippocampus, thalamus and striatum in TgHD minipigs *in vivo* by using ^{1}H MRS. Single voxel spectroscopy revealed significant increase of the tCho/tCr and tNAA/tCr ratios in WM of TgHD animals. These changes are probably generated by decreased tCr concentration even when its change alone is not significant in absolute terms, since the difference in absolute tNAA and tCho concentrations are minimal. Increase of the tNAA/tCr ratio apparently originates from reduced tCr concentration because tNAA increase is unlikely.

A raised choline concentration might also be responsible for an increase of tCho/tCr ratio in WM of TgHD animals. Indeed, increase of tCho has been connected with myelin breakdown (Pouwels *et al.* 1998, Zacharoff *et al.* 2012) and diffusion tensor imaging (DTI) studies in early stage of HD suggested axonal injury and demyelination process in WM (Rosas *et al.* 2006, Weaver *et al.* 2009) which might also explain our observation.

It should be noted that a rectangular region of interest (ROI) was not placed in the white matter exclusively but involved also adjacent structures. We assume that a substantial part of the signal measured by SVS MRS in the white matter originated from the cingulate cortex area. With regard to placement of ROI and precision of the measurement, we did not detect changes found in posterior cingulate cortex by Unschuld at al. (Unschuld *et al.* 2012), who showed a NAA concentration decline and a lower level of glutamate concentration in posterior cingulate cortex in individuals with the HD mutation.

Although a decrease of tCr concentration in the gray matter in HD patients was reported in several publications (Sturrock *et al.* 2010, van den Bogaard *et al.* 2011), a decrease in tCr or changes in the metabolite/tCr ratios in WM of TgHD minipigs, before onset of neurological deficit, represents a new piece of information.

Similarly, 2D-CSI revealed a decrease in tCr (absolute concentration) in the thalamus, and also a significantly increased tCho/tCr ratio in all examined areas (striatum, thalamus and hippocampus) of transgenic animals. We also observed significant elevation of the tNAA/tCr and Glx/tCr ratios in the thalamus and of Ins/tCr in hippocampus. All these changes can be explained by a decrease of tCr.

Creatine is an important marker for brain energy metabolism. Lower creatine levels were reported in striatum of HD patients suggesting impaired energy metabolism (van den Bogaard *et al.* 2011). In the brain of R6/2 mouse Zacharoff et al. observed the elevations of Cr and PCr between 4 and 8 weeks without further significant changes. They suggested that these changes stem from early stages of the disease (Zacharoff *et al.* 2012).

We found a decrease in tCr similar to observations in human HD studies (van den Bogaard *et al.* 2011, Sturrock *et al.* 2010), although in a different brain structure (thalamus). The significant elevation of tCho/tCr in all examined areas may also indicate a decrease of tCr. We may therefore agree with Zacharoff's hypothesis that the changes in Cr and PCr

concentrations are related to early stages of HD, although the experiments of Zacharoff *et al*. 2012, done on R6/2 mice, revealed increased concentrations contrary to our findings.

Changes in the choline concentrations are generally associated with modifications of membrane composition. An increased choline signal was found in Alzheimer's disease or in multiple sclerosis (Govindaraju *et al.* 2000), but also in HD (Sturrock *et al.* 2010). Hence an increase of tCho/tCr ratio might be also caused by raised choline concentration.

During HD progression alterations of concentrations of tNAA, Glx and Ins were reported (Sturrock *et al.* 2010, van den Bogaard *et al.* 2011).

tNAA concentration within gray matter indicates neuronal abundance and viability (Sturrock *et al.* 2010). Myo-inositol primarily located within astrocytes is considered a gliosis marker (Castillo *et al.* 2000, Zacharoff *et al.* 2012). Glutamine concentration may increase with gliosis and both glutamine and glutamate can act as osmolytes (Zacharoff *et al.* 2012).

Although we detected a slight non-significant decrease in absolute concentration of tNAA in two–year–old TgHD animals, we did not observe significant changes in absolute concentration values as such and changes of metabolic ratios may be predominantly attributed to decrease of tCr associated to changes in energy metabolism rather than to changes in concentration of tNAA, Glx or Ins.

It should be also noted that HD and control minipigs may react differently to anesthesia, nevertheless similar SDs of average values of metabolite concentrations in both groups indicate that possible differences caused by anesthesia are small and can be neglected.

Default LCModel water concentration and relaxation times for the human brain were used for the calculation of metabolite concentrations. The missing brain tissue segmentation accounting for different water signal contributions of white and gray matter as well as possibly biased relaxation times of both water compartments may lead to systematic shifts in estimated metabolite concentrations. However, since the best effort has been made to keep the

VOI position in individual examinations constant the systematic shifts in concentrations were minimized.

The dependence on the water signal is canceled out by the calculation of concentration ratios, i.e., the concentrations were related to tCr. Nevertheless, the resulting concentration ratios may be also influenced by different concentrations of tCr in the white and gray matter. However, based on the presented results the authors believe that the observed changes in metabolite concentrations/ratios can be ascribed to physiological/biochemical tissue changes as described above.

Conclusion

We found a significant decrease of total creatine concentration in the thalamus and increased metabolic ratios tCho/tCr in the striatum, thalamus, hippocampus as well as white matter of transgenic minipigs before clinical pathology onset. Similarly, increased tNAA/tCr and Glx/tCr ratios were observed in the thalamus. We hypothesized that the majority of the observed changes are predominantly related to changes in energy metabolism.

Conflict of interest

The authors declare that they have no conflict of interest.

Acknowledgement

The authors would like to thank Tibor Liptaj and Svatava Kasparova for their support and Michal Kalinak and Michael Kenneth Lawson for revision of the manuscript.

This study was supported by the MH CZ-DRO („Institute for Clinical and Experimental Medicine – IKEM, IN 00023001“), CHDI Foundation (A-5378 , A-8248), TA01011466, 7F - Finanční mechanismy EHP/Norsko (2008-2017) 7F14308, EXAM - CZ.1.05./2.1.00/03.0124, and RVO: 67985904

References

BANO D, ZANETTI F, MENDE Y, and NICOTERA P: Neurodegenerative processes in Huntington's disease. *Cell Death Dis.* **2**: e228, 2011.

BAXA M, HRUSKA-PLOCHAN M, JUHAS S, VODICKA P, and PAVLOK A: A Transgenic Minipig Model of Huntington's Disease. *J. Huntingtons. Dis.* **2**: 47–68, 2013.

BENOVA I, KUPCOVA SKALNIKOVA H, KLIMA J, JUHAS S, and MOTLIK J: C03 Activation of cytokine production in F1 and F2 generation of miniature pigs transgenic for N-terminal part of mutated human huntingtin. *J. Neurol. Neurosurg. Psychiatry* **83**: A16–A16, 2012.

VAN DEN BOGAARD SJA, DUMAS EM, TEEUWISSE WM, KAN HE, WEBB A, ROOS RAC, and VAN DER GROND J: Exploratory 7-Tesla magnetic resonance spectroscopy in Huntington's disease provides in vivo evidence for impaired energy metabolism. *J. Neurol.* **258**: 2230–2239, 2011.

BOHANNA I, GEORGIOU-KARISTIANIS N, HANNAN AJ, and EGAN GF: Magnetic resonance imaging as an approach towards identifying neuropathological biomarkers for Huntington's disease. *Brain Res. Rev.* **58**: 209–225, 2008.

CASTILLO M, SMITH JK, and KWOCK L: Correlation of myo-inositol levels and grading of cerebral astrocytomas. *AJNR. Am. J. Neuroradiol.* **21**: 1645–1649, 2000.

GÓMEZ-ANSÓN B, ALEGRET M, MUÑOZ E, SAINZ A, MONTE GC, and TOLOSA E: Decreased frontal choline and neuropsychological performance in preclinical Huntington disease. *Neurology* **68**: 906–910, 2007.

GOVINDARAJU V, YOUNG K, and MAUDSLEY AA: Proton NMR chemical shifts and coupling constants for brain metabolites. *NMR Biomed.* **13**: 129–153, 2000.

HEIKKINEN T, LEHTIMÄKI K, VARTIAINEN N, PUOLIVÄLI J, HENDRICKS SJ, GLASER JR, BRADAIA A, WADEL K, TOULLER C, KONTKANEN O, et al.:

Characterization of neurophysiological and behavioral changes, MRI brain volumetry and 1H MRS in zQ175 knock-in mouse model of Huntington's disease. *PLoS One* **7**: e50717, 2012.

HENRY P-G, and MOCHEL F: The search for sensitive biomarkers in presymptomatic Huntington disease. *J. Cereb. Blood Flow Metab.* **32**: 769–770, 2012.

JENKINS BG, ANDREASSEN OA, DEDEOGLU A, LEAVITT B, HAYDEN M, BORCHELT D, ROSS CA, FERRANTE RJ, and BEAL MF: Effects of CAG repeat length, HTT protein length and protein context on cerebral metabolism measured using magnetic resonance spectroscopy in transgenic mouse models of Huntington's disease. *J. Neurochem.* **95**: 553–562, 2005.

JIRU F, SKOCH A, WAGNEROVA D, DEZORTOVA M, and HAJEK M: jSIPRO - analysis tool for magnetic resonance spectroscopic imaging. *Comput. Methods Programs Biomed.* **112**: 173–188, 2013.

MACAKOVA M, HANSIKOVA H, ANTONIN P, HAJKOVA Z, SADKOVA J, JUHA S, JUHASOVA J, BAXA M, ZEMAN J, and MOTLIK J: C04 Reproductive parameters and mitochondrial function in spermatozoa of F1 and F2 minipig boars transgenic for n-terminal part of the human mutated huntingtin. *J. Neurol. Neurosurg. Psychiatry* **83**: A16–A16, 2012.

MORTON a J, and HOWLAND DS: Large genetic animal models of Huntington's disease. *J. Huntingtons. Dis.* **2**: 3–19, 2013.

VAN OOSTROM JCH, SIJENS PE, ROOS RAC, and LEENDERS KL: 1H magnetic resonance spectroscopy in preclinical Huntington disease. *Brain Res.* **1168**: 67–71, 2007.

PEREZ-DE LA CRUZ V, and SANTAMARIA A: Integrative hypothesis for Huntington's disease: a brief review of experimental evidence. *Physiol. Res* 513–526, 2007.

POUWELS PJ, KRUSE B, KORENKE GC, MAO X, HANEFELD FA, and FRAHM J: Quantitative proton magnetic resonance spectroscopy of childhood adrenoleukodystrophy. *Neuropediatrics* **29**: 254–264, 1998.

PROVENCHER SW: Estimation of metabolite concentrations from localized in vivo proton NMR spectra. *Magn. Reson. Med.* **30**: 672–679, 1993.

REYNOLDS NC, PROST RW, and MARK LP: Heterogeneity in 1H-MRS profiles of presymptomatic and early manifest Huntington's disease. *Brain Res.* **1031**: 82–89, 2005.

ROSAS HD, TUCH DS, HEVELONE ND, ZALETA AK, VANGEL M, HERSCH SM, and SALAT DH: Diffusion tensor imaging in presymptomatic and early Huntington's disease: Selective white matter pathology and its relationship to clinical measures. *Mov. Disord.* **21**: 1317–1325, 2006.

ROTONDO E, BRUSCHETTA G, SACCÀ A, BRAMANTI P, and DI PASQUALE MR: Straightforward relative quantitation and age-related human standards of N-acetylaspartate at the centrum semiovale level by CSI 1H-MRS. *Magn. Reson. Imaging* **21**: 1055–1060, 2003.

STURROCK A, LAULE C, DECOLONGON J, DAR SANTOS R, COLEMAN AJ, CREIGHTON S, BECHTEL N, REILMANN R, HAYDEN MR, TABRIZI SJ, et al.: Magnetic resonance spectroscopy biomarkers in premanifest and early Huntington disease. *Neurology* **75**: 1702–1710, 2010.

SUNDGREN PC, JENNINGS J, ATTWOOD JT, NAN B, GEBARSKI S, MCCUNE WJ, PANG Y, and MALY P: MRI and 2D-CSI MR spectroscopy of the brain in the evaluation of patients with acute onset of neuropsychiatric systemic lupus erythematosus. *Neuroradiology* **47**: 576–585, 2005.

TKAC I, HENRY P-G, ZACHAROFF L, WEDEL M, GONG W, DEELCHAND DK, LI T, and DUBINSKY JM: Homeostatic adaptations in brain energy metabolism in mouse models of Huntington disease. *J. Cereb. Blood Flow Metab.* **32**: 1977–1988, 2012.

UNSCHULD PG, EDDEN RAE, CARASS A, LIU X, SHANAHAN M, WANG X, OISHI K, BRANDT J, BASSETT SS, REDGRAVE GW, et al.: Brain metabolite alterations and cognitive dysfunction in early Huntington's disease. *Mov. Disord.* **27**: 895–902, 2012.

WEAVER KE, RICHARDS TL, LIANG O, LAURINO MY, SAMII A, and AYLWARD EH: Longitudinal diffusion tensor imaging in Huntington's Disease. *Exp. Neurol.* **216**: 525–529, 2009.

ZACHAROFF L, TKAC I, SONG Q, TANG C, BOLAN PJ, MANGIA S, HENRY P-G, LI T, and DUBINSKY JM: Cortical metabolites as biomarkers in the R6/2 model of Huntington's disease. *J. Cereb. Blood Flow Metab.* **32**: 502–514, 2012.

ZUCCATO C, VALENZA M, and CATTANEO E: Molecular Mechanisms and Potential Therapeutical Targets in Huntington ' s Disease. *Physiol. Rev.* **90**: 905–981, 2010.

Table 1: Concentrations of metabolites and the ratios of metabolite concentrations to tCr in the white matter (average values ± standard deviation). Significance level * $p<0.05$, ** $p<0.005$.

	metabolite concentrations					**ratios**			
	tNAA [mmol/kg]	**tCr [mmol/kg]**	**tCho [mmol/kg]**	**Glx [mmol/kg]**	**Ins [mmol/kg]**	**tNAA/tCr**	**tCho/tCr**	**Glx/tCr**	**Ins/tCr**
controls	5.5±0.4	4.1±0.6	1.4±0.2	9.2±2.2	4.4±1.0	1.4±0.1	0.35±0.04	2.3±0.8	1.1±0.3
HD	5.5±0.9	3.7±0.8	1.6±0.3	9.4±0.9	4.4±1.2	1.6±0.1*	0.47±0.06**	2.7±0.3	1.3±0.4

Table 2: Concentrations of metabolites and the ratios of metabolite concentrations to tCr in striatum, thalamus and hippocampus (average values ± standard deviation). Significance level * $p<0.05$, ** $p<0.005$.

	metabolite concetrations					**ratios**			
	tNAA [mmol/kg]	**tCr [mmol/kg]**	**tCho [mmol/kg]**	**Glx [mmol/kg]**	**Ins [mmol/kg]**	**tNAA/tCr**	**tCho/tCr**	**Glx/tCr**	**Ins/tCr**
	striatum								
controls	5.4±0.3	5.4±0.5	2.19±0.24	11.4±1.1	5.3±0.6	1.01±0.09	0.41±0.03	2.1±0.3	0.99±0.13
HD	5.1±0.4	4.7±0.6	2.11±0.28	10.9±1.6	4.8±0.6	1.09±0.09	0.45±0.01*	2.4±0.4	1.02±0.04
	thalamus								
controls	5.4±0.6	4.9±0.4	1.89±0.09	10.2±1.1	4.8±0.8	1.12±0.13	0.39±0.03	2.1±0.3	0.98±0.15
HD	5.3±0.3	4.2±0.2**	1.81±0.07	10.1±0.9	4.7±0.5	1.28±0.10*	0.44±0.02*	2.5±0.2*	1.12±0.11
	hippocampus								
controls	4.8±1.0	4.5±0.9	1.66±0.18	9.5±1.4	4.9±1.1	1.09±0.19	0.38±0.05	2.2±0.7	1.10±0.12
HD	4.4±0.7	3.5±0.6	1.58±0.17	10.3±0.9	4.9±0.4	1.26±0.16	0.45±0.04*	3.0±0.5	1.44±0.28*

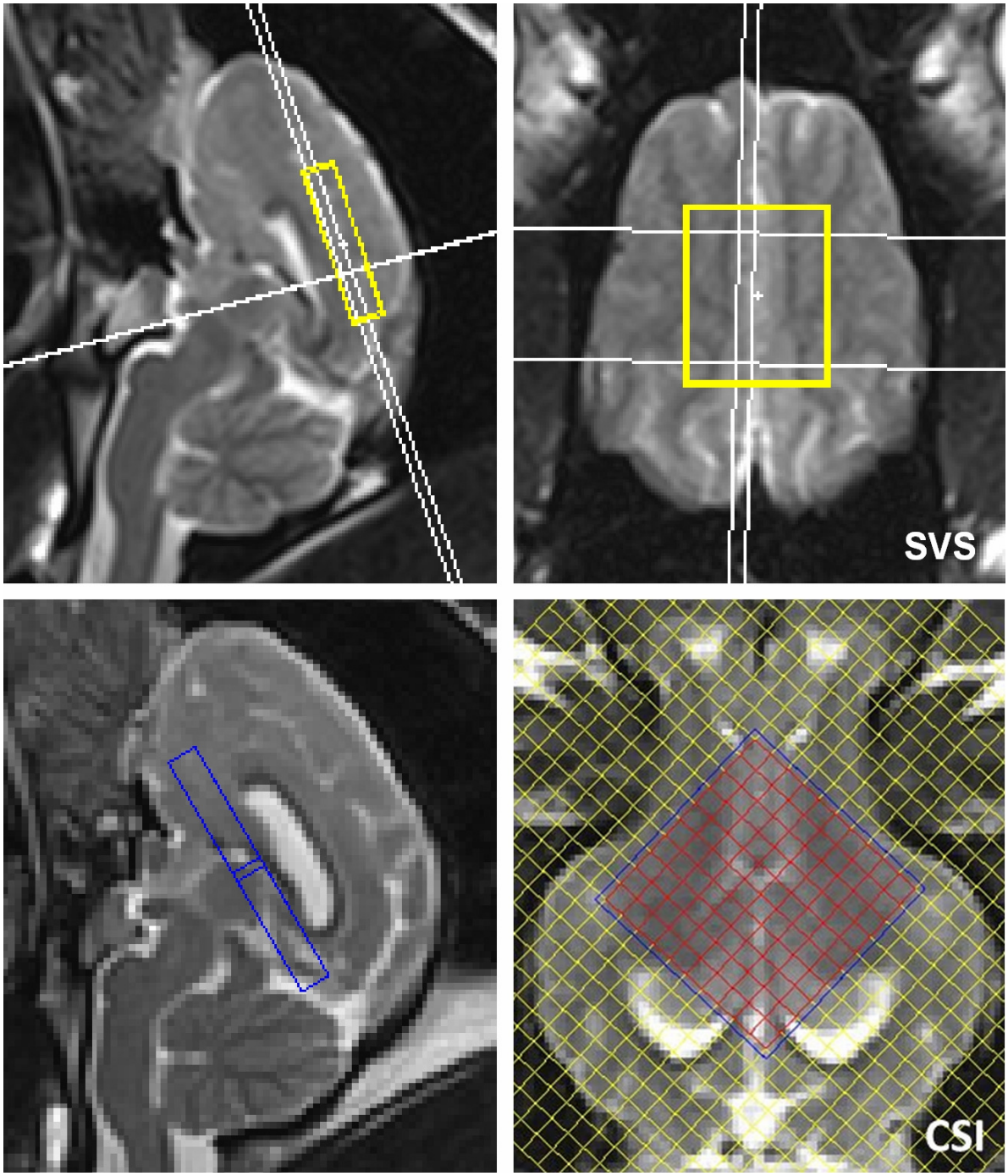

Figure 1: The position of the voxels in the white matter (SVS), and in the striatum, thalamus and hippocampus (2D-CSI, a spectroscopic grid after zero filling is shown).

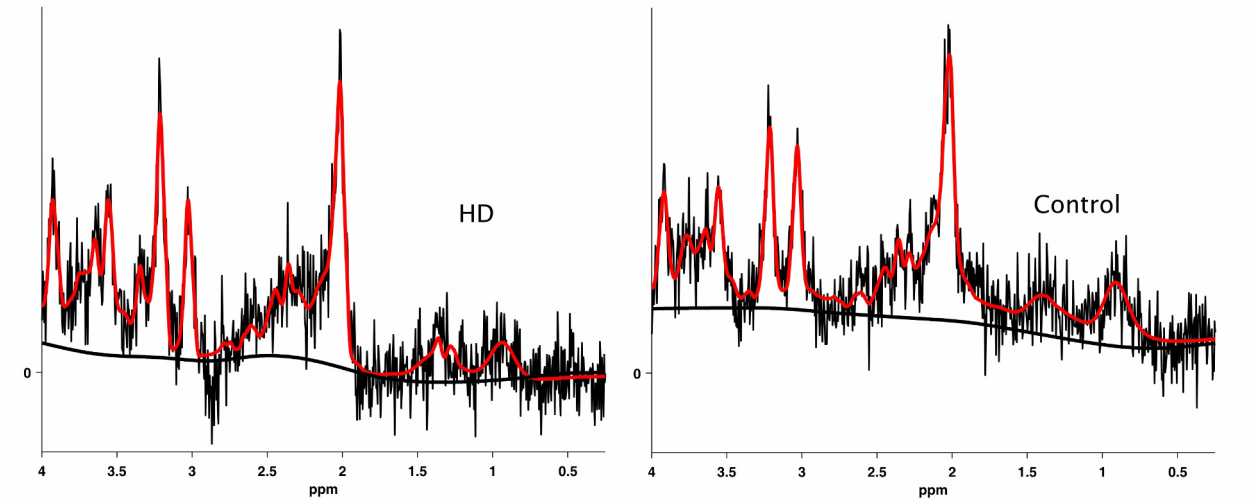

Figure 2: Representative SVS spectra from white matter of HD (left) and control (right) minipig. No FID filtering or line broadening was used.

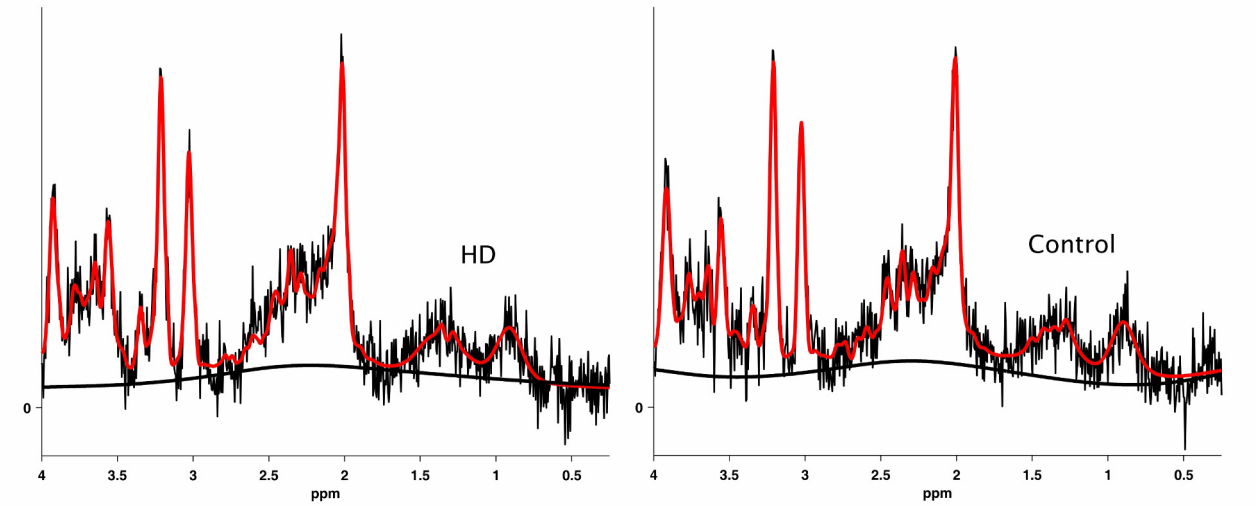

Figure 3: Representative spectrum in one interpolated voxel (2.8x2.8x5.0 mm) of thalamus from HD (left) and control (right) minipig measured by 2D-CSI. No FID filtering or line broadening was used.